

Research Article

Effect of Ni on graphene supported Pt–Ru binary catalyst for borohydride electro-oxidation

M. Elumalai¹, S. Kiruthika², B. Muthukumar^{1,*}

¹Department of Chemistry, Presidency College, Chennai – 600 005, India.

²Department of Chemical Engineering, SRM University, Chennai – 603 203, India.

*Corresponding author's e-mail: dr.muthukumar@yahoo.com

Abstract

Catalysts of Pt–Ni, Pt–Ru and Pt–Ru–Ni supported on graphene are prepared using Bonnemann reduction method to study the electro-oxidation of sodium borohydride in membraneless fuel cell. The prepared electrocatalysts were characterized by transmission electron microscopy (TEM), energy dispersive X-ray spectroscopy (EDX) and X-ray diffraction (XRD) analyses. The synthesized catalysts had similar particle morphology, and their particle sizes were 3-5 nm. The electrocatalytic activities were examined by cyclic voltammetry (CV) and chronoamperometry (CA). The electrochemical results obtained at room temperature indicated that the ternary Pt–Ru–Ni/G (60:30:10) catalyst displayed better catalytic activity for sodium borohydride oxidation compared with the other prepared catalysts. During the experiments performed on single membraneless fuel cell, Pt–Ru–Ni/G (60:30:10) performed better among all the catalysts prepared with power density of 35.61 mWcm^{-2} . The better performance of ternary Pt–Ru–Ni/G catalysts may be due to the formation of a ternary alloy and the smaller particle size.

Keywords: Sodium borohydride; Graphene support; Power density; Ternary alloy catalyst; Membraneless borohydride fuel cell.

Introduction

In recent years, fuel cells have not only emerged to offer great opportunities for cleaner more sustainable energy, but also to fulfill the increasing energy needs. Among the various kinds of fuel cells, membraneless fuel cell is considered as a promising candidate for miniature appliances [1–4]. Membraneless fuel cell is a device that incorporated into single micro structured manifold using all the fundamental components of the fuel cells. Membraneless fuel cells also called laminar flow-based fuel cells eliminate the expenditure of proton exchange membrane as they utilize the co-laminar flow nature of multistream in a single microfluidic channel to separate the fuel and an oxidant. [5–7]. Membraneless fuel cells overwhelmed many problems associated with polymer electrolyte membrane-based fuel cells such as membrane degradation, humidification, fuel crossover, and water management [8].

Supporting material significantly affects the catalytic characteristics of Pt-based electrocatalysts. Mostly, carbon materials have been

investigated as catalyst supports for fuel cells, such as Vulcan XC-72R carbon [9, 10], carbon nanotubes (CNTs) [11], carbon nanofibers [12], graphene [13], and mesoporous carbon [14, 15]. Among these materials, graphene has attracted considerable interests over the last few years, because of its unique and outstanding physicochemical properties, such as fast charge transport mobility, good transparency, great mechanical flexibility, astonishing elastic properties, and a huge specific surface area (Theoretically $2630 \text{ m}^2 \text{ g}^{-1}$ for a single layer) (Fig.1) [16–18].

Sodium borohydride, one of the most promising combusting materials, is widely used in microfluidic fuel cells, due to its facile electro-oxidation on Pt catalyst. However, borohydride electro-oxidation on pure platinum encounters many problems such as the difficulties that sodium borohydride hydrolysis and the formation of hydroxyborohydride ion (BH_3OH^-) intermediate that affect the Pt anode catalysts performance [19]. In order to improve the catalytic activity, a second metal is introduced as a co-catalyst with Pt metal, for

example Pt–Ru, Pt–Ni, Pt–Co, Pt–Sn, and Pt–Cu [2–5, 18].

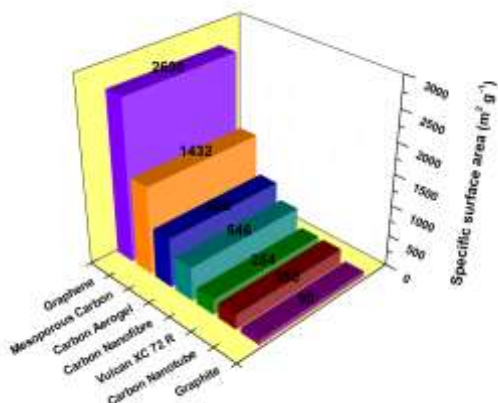


Fig. 1. Shows the specific surface area of different carbon supporting materials

Among the binary catalysts, Pt–Ru/C is found to be more active than other catalysts for sodium borohydride electro-oxidation [20]. Vincent W. S. Lam et al, have shown that the addition of Ru contributes to the formation of a more selective catalyst for the oxidation of sodium borohydride. The performance of Pt–Ru/C electrocatalyst also depends greatly on the ratio of Pt:Ru atoms and its preparation procedure. To further improve Pt–Ru electrocatalysts activity, Ni is introduced as a third metal in the Pt–Ru catalyst composition. This helps to enhance the dehydrogenation reaction during the oxidation of sodium borohydride. Many researchers studied that Ni can modify the behavior of the Pt–Ru/C electrocatalyst and act as an assistant component [21, 22]. The main advantage of the introduction of Ni is to minimize the oxidation potential of sodium borohydride intermediate, coupled with the rise in current density. Therefore, the addition of Ni into Pt–Ru binary catalyst in the MLBFC would thus increase the borohydride electro-oxidation reaction.

In our study Pt/G (100), Pt–Ni/G (50:50), Pt–Ru/G (50:50) and Pt–Ru–Ni/G (60:30:10) catalysts were prepared by using Bonnemann method from their precursors to sodium borohydride electro-oxidation. The prepared electrocatalysts are characterized using transmission electron microscope (TEM), energy dispersive X-ray (EDX) analysis and X-ray diffraction (XRD) analysis. Sodium borohydride in the presence of above catalysts was studied using cyclic voltammetry (CV) and chronoamperometry (CA). Eventually, the catalysts were tested as an anode in MLBFC.

Materials and methods

Materials and reagent

The following metal precursors $\text{H}_2\text{PtCl}_6 \cdot 6\text{H}_2\text{O}$ (from Aldrich), $\text{RuCl}_3 \cdot 3\text{H}_2\text{O}$ (from Merck) and $\text{NiCl}_2 \cdot 6\text{H}_2\text{O}$ (from Sigma Aldrich) were used to synthesis the electrocatalysts. Graphene (purity of 97%, from Graphene Supermarket Supply) was used as support for the catalysts. Graphite Plates (3 cm long and 0.1 cm wide, from E-TEK) were used as substrates for the catalyst to prepare the electrodes. Nafion[®] (DE 521, Dupont USA) dispersion was used to prepare the catalyst slurry. Tetrahydrofuran (THF) (from Merck) was used as a solvent. Sodium Borohydride (from Merck) in Sodium hydroxide (from Merck), and sodium perborate (from Riedel) in H_2SO_4 (from Merck) were used as the fuel, and oxidant respectively. All the chemicals were of analytical grade. Pt/G (40-wt%, from E-TEK) was used as the cathode catalyst.

Catalyst preparation

Bonnemann Method: The colloidal metals were synthesized by colloidal metal preparation technique so-called Bonneman method, according to the variant described by Gotze and Wendt [23] in the Bonneman method hydro-triorganoborates with tetraalkylammonium cations act as both reductant and colloidal particle encapsulating agent, respectively. The Bonnemann method was chosen as crystallite sizes between 3–5 nm can be obtained, showing enhanced electrocatalytic activities due to their favorable surface to bulk ratio. First tetraalkylammonium cation prepared via the reduction of anhydrous $\text{H}_2\text{PtCl}_6 \cdot 6\text{H}_2\text{O}$, $\text{RuCl}_3 \cdot 3\text{H}_2\text{O}$ and $\text{NiCl}_2 \cdot 6\text{H}_2\text{O}$ dissolved in tetrahydrofuran (THF). Then a suspension of graphene, in ultrapure water (Millipore MilliQ, 18MQcm) was impregnated with the appropriate amount of the colloidal solution. Thermal treatments were carried out in a H_2 reducing atmosphere at 300°C for 120 min (Fig. 2). For comparison, the monometallic Pt/G, bimetallic Pt–Ru/G and Pt–Ni/G were synthesized under the same conditions. The electrocatalytic mixtures and atomic ratio was Pt/G (100), Pt–Ni/G (50:50), Pt–Ru/G (50:50), Pt–Ru–Ni/G (60:30:10). The nominal loading of metals in the electrocatalysts was 40%wt and rest 60% wt. was graphene.

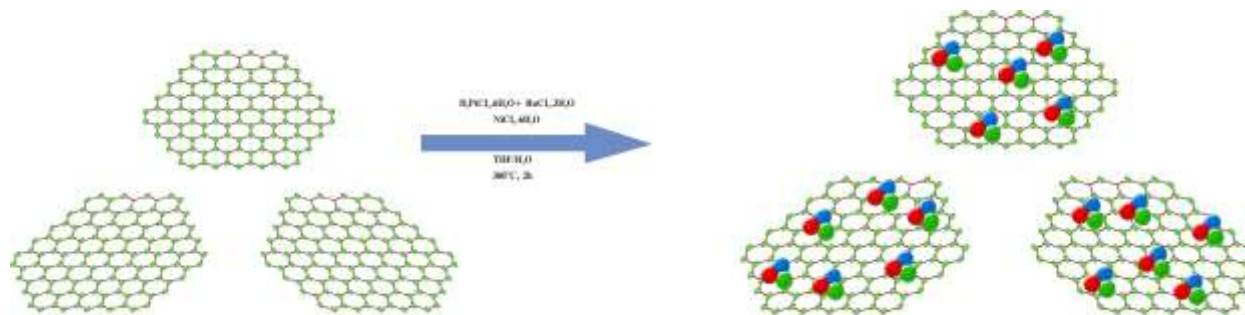


Fig. 2. Schematic of preparation of graphene supported Pt–Ru–Ni catalysts

Physical characterization

The particle size distribution and mean particle size were evaluated using TEM (Philips CM 12 Transmission Electron Microscope). The crystal structure of the prepared electrocatalysts was examined by powder X-ray diffraction (XRD) using a Rigaku multiflex diffractometer (model RU-200 B) with Cu–K α radiation source ($\lambda_{K\alpha 1} = 1.5406 \text{ \AA}$) operating at room temperature. The tube current was 40 mA with a tube voltage of 40 kV. The 2θ angular positions between 20° and 90° were recorded at a scan rate 5° min^{-1} the mean particle size analyzed from TEM is proved by determining the crystallite size from XRD pattern using “Scherer” formula. Pt (2 2 0) diffraction peak was selected to calculate crystallite size and lattice parameter of platinum. According to Scherrer’s equation (1) [25].

$$d = \frac{0.9\lambda_{K\alpha 1}}{\beta_{2\theta} \cos \theta_{\max}} \quad (1)$$

Where D is the average crystallite size, θ_{\max} is the angle at the position of the peak maximum, $\beta_{2\theta}$ is the half width of the peak (in radians), 0.9 is the shape factor for spherical crystallite and $\lambda_{K\alpha 1}$ is the wavelength of X-rays used. The lattice parameters of the catalysts were estimated according to equation (2) [25].

$$a = \frac{\sqrt{2} \lambda_{K\alpha 1}}{\sin \theta_{\max}} \quad (2)$$

Where a is the lattice parameter (nm) and all the other symbols have the same meanings as in equation 1. The atomic ratios of the synthesized electrocatalysts were determined by an energy dispersive X-ray (EDX) analyzer, which was cohesive with the TEM instrument.

Electrochemical Measurement

Electrochemical Measurements were performed on an electrochemical workstation (CH Instruments, Model CHI6650, USA)

interfaced with a personal computer using the CHI software, at room temperature. A common three-electrode electrochemical cell using cyclic voltammetry (CV) and Chronoamperometry (CA) techniques was used for measurements. Catalysts coated glassy carbon electrode (GCE, 3 mm diameter and 0.071 cm^2 of electrode area, from CHI, USA) was used as the working electrode and platinum foil was used as the counter electrode. Ag/AgCl in saturated KCl was used as the reference electrode. The working electrode was prepared by applying catalyst ink made of 20 mg of electrocatalyst in a solution of 50 mL of water containing three drops of 6% PTFE suspension. The resulting mixture was treated in an ultrasound bath for 10 min to get a even dispersion. The catalyst slurry was then drop-cast on to a glassy carbon electrode and allowed to dry at 100°C for 30 min for assessing the electrocatalytic activity of the working electrode; cyclic voltammetry was obtained in 0.15 M sodium borohydride and 3 M NaOH solution with a scan rate of 50 mV S^{-1} . For the durability test, the chronoamperometric experiments were carried out from the potential step of -1.2 to -0.2 V for 600 s in the same electrolyte. Before each measurement, the solution was purged with high-purity N_2 gas for at least 30 min to ensure oxygen-free measurements.

Results and discussions

Physical Characterization

X-ray Diffraction (XRD)

The XRD patterns of the prepared Pt–Ni/G (50:50), Pt–Ru/G (50:50) and Pt–Ru–Ni/G (60:30:10) catalysts are shown in fig.3. The diffraction peaks seen in all the diffraction patterns at around 25° – 30° are associated with (0 0 2) plane of hexagonal structure of graphene support. The diffractogram of Pt/G electrocatalyst show peaks at around 40° , 47° ,

67° and 82°, which are related with the (1 1 1), (2 0 0), (2 2 0) and (3 1 1) crystalline planes of the face centered cubic (fcc) structure characteristic of platinum and platinum alloys.

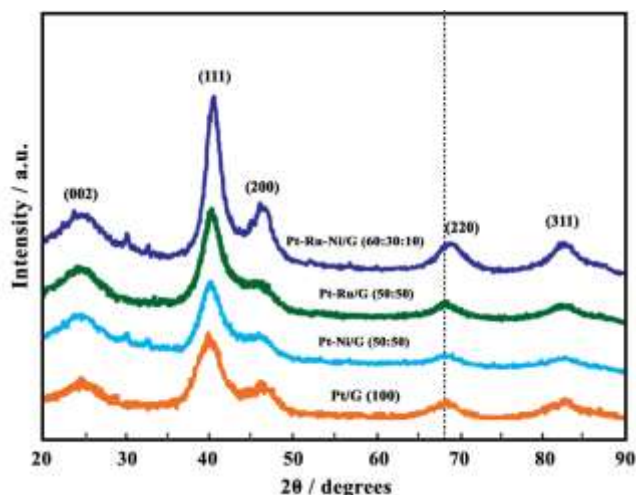


Fig. 3. X-ray diffraction patterns of Pt–Ru–Ni/G (60:30:10), Pt–Ni/G (50:50), Pt–Ru/G (50:50) and Pt/G (100) catalysts

Comparing with the reflections of pure Pt, the diffraction peaks for the Pt–Ru, Pt–Ni, and Pt–Ru–Ni catalysts are shifted slightly to a higher 2θ values. The slight shifts of the diffraction peaks expose the formation of an alloy involving the incorporation of Ru and Ni atoms into the fcc structure of Pt. It is important to note that no diffraction peaks, indicating the existence of either pure Ru and Ni or Ru-rich hexagonal close packed (hcp) phase, and Ni oxide, appear. The lattice parameters of Pt–Ru/G, Pt–Ni/G and Pt–Ru–Ni/G catalysts, which reflect the formation of a solid solution and be calculated by using the Pt (2 2 0) crystal faces, are given in Table 1. The lattice parameters obtained for the Pt–Ni/G, Pt–Ru/G, and Pt–Ru–Ni/G catalysts are smaller than those for Pt/G. In fact, the decrease in lattice parameters of the alloy catalysts reflects the progressive increase in the incorporation of Ru and Ni into the alloy state. Among four catalysts, the lattice parameter for Pt–Ru–Ni/G is the

smallest, while that for Pt/G is the biggest. The average particle size d may be estimated from full width at half-maximum (FWHM) of Pt (2 2 0) according to “Debye-Scherrer formula” [26, 27].

Transmission Electron Microscopy (TEM)

The TEM images and histogram of particle size of the Pt/G, Pt–Ru/G and Pt–Ni/G and Pt–Ru–Ni/G catalysts are presented in fig. 4a-c, and 4d-f respectively. The metal particles on all the catalysts are spherical in shape and are highly dispersed on the graphene support without severe aggregation. The heavy black dots on the graphene support are the catalyst particles. The average size of the metal particles on the prepared catalysts was assessed from an ensemble of 200 particles in an arbitrarily selected area of the corresponding TEM images. In comparison to Pt–Ru/G (50:50), Pt–Ni/G (50:50) and Pt–Ru–Ni/G (50:40:10) the mean particle size of Pt–Ru–Ni/G (60:30:10) were smaller. The particle size for distribution of these catalysts is shown in Table 1 in accordance to TEM images. The particle size for Pt–Ru–Ni/G (60:30:10) varies from 3 to 4 nm, with a mean diameter of 3.4 nm. In the size of 1 to 5 nm, the mean particle size for Pt–Ru–Ni/G (50:40:10) and Pt–Ru–Ni/G (60:30:10) is 3.9 nm and 3.4 nm respectively. The mean particle size found by TEM images and XRD analysis were similar. Further, it was observed that the particle size of Pt–Ru/G (50:50) was similar to that of Pt–Ni/G (50:50).

Energy Dispersive X-ray (EDX) Analysis

The EDX analyses of all the Pt/G, Pt–Ni/G, Pt–Ru/G, and Pt–Ru–Ni/G catalysts are shown in fig. 5. Fig. 5 a-d indicates the presence of Pt and carbon; Pt, Ru and carbon; Pt, Ni and Carbon; and both the combinations of Pt, Ru, Ni and Carbon, respectively. The EDX results are shown in Table 1.

Table 1. The EDX compositions, lattice parameters and the particle size obtained for different atomic ratios of electrocatalysts.

Electrocatalysts	Nominal atomic ratio			EDX atomic ratio			lattice parameters (nm)	Crystallite size (nm)	Particle size from TEM (nm)
	Pt	Ru	Ni	Pt	Ru	Ni			
Pt/G	100	–	–	99	–	–	0.3919	4.9	4.7
Pt–Ni/G	50	–	50	51	–	49	0.3898	4.7	4.5
Pt–Ru/G	50	50	–	52	48	–	0.3899	4.6	4.3
Pt–Ru–Ni/G	60	30	10	62	29	09	0.3895	3.7	3.4

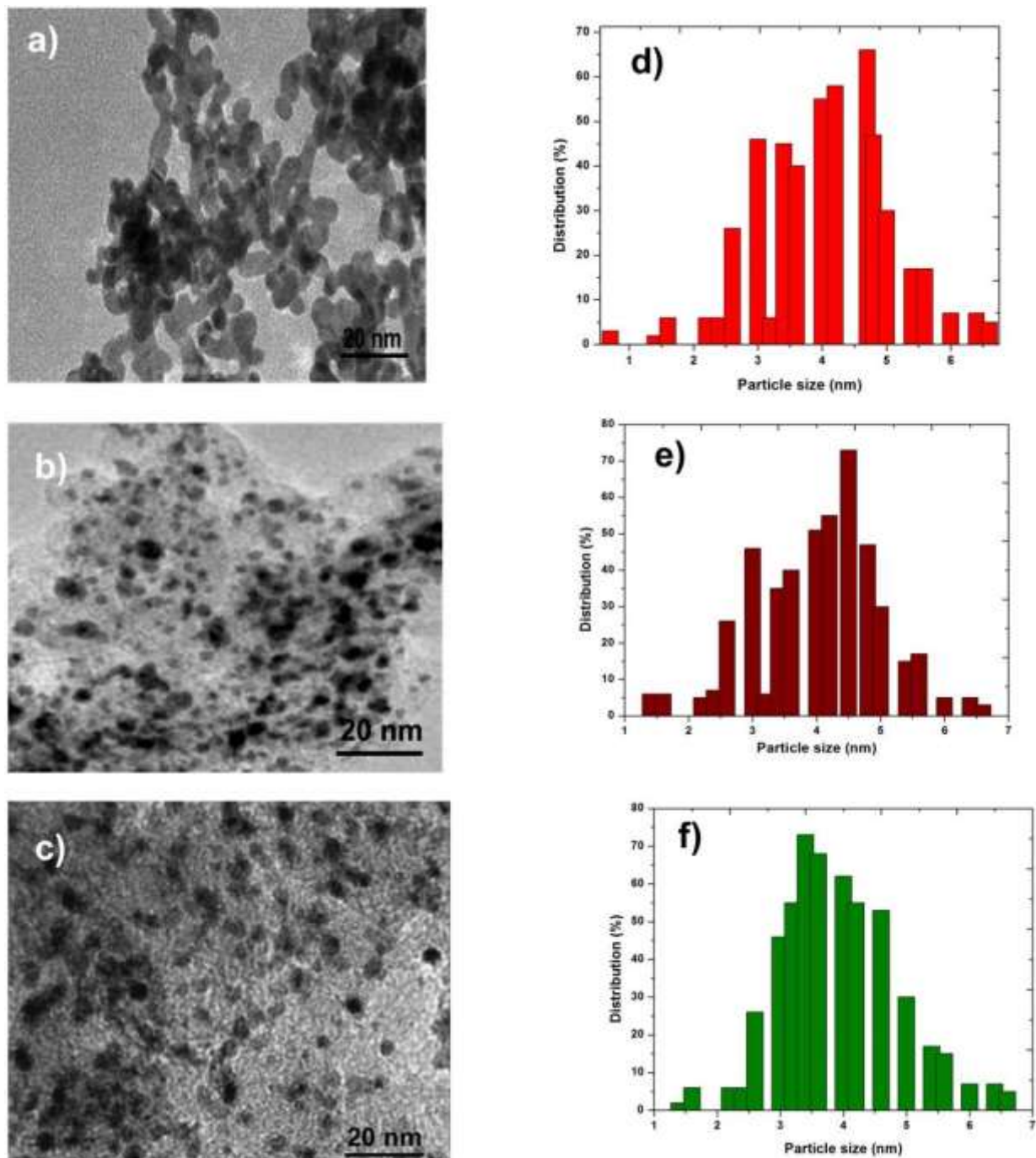


Fig. 4 (a-c). TEM images and d-f) particle size of Pt/G, Pt–Ni/G and Pt–Ru–Ni/G catalysts

The catalysts prepared had the desired elements with some variation in composition. The EDX results of the binary Pt–Ru/G and Pt–Ni/G and the ternary Pt–Ru–Ni/G catalysts are very close to the nominal values, which indicate that the metals were loaded onto the graphene support without obvious loss.

Electrochemical characterization

CO stripping voltammetry

To investigate the catalytic of synthesized electrocatalysts supported on graphene for borohydride oxidation reaction and the performance of MLBFC, CO_{ads} stripping

voltammograms were conducted in 0.5 M H₂SO₄ at room temperature. Fig. 6 shows the CO_{ads} stripping voltammograms of Pt–Ru–Ni/G (60:30:10), Pt–Ru/G (50:50), Pt–Ni/G (50:50) and Pt/G (100) electrocatalysts at a CO adsorption potential of 0.07 V and a sweep rate of 50 mV s⁻¹ between 0.05 V and 0.9 V versus Ag/AgCl. These conditions allowed elimination of all adsorbed CO during the first cycle, and the current in second cycle coincided with the baseline in the case of pure supporting electrolyte. The CO_{ads} oxidation peaks of the graphene substrate were observed at 0.35, 0.25, and 0.2 V vs. Ag/AgCl, for Pt/G, Pt–M/G (M = Ni and Ru) and Pt–Ru–Ni/G electrocatalysts,

respectively. For the Pt–Ru–Ni/G electrocatalysts, there was a cathodic shift of at least 150 mV because of CO oxidation, compared to Pt/G. The peak positions in the voltammograms of the bimetallic Pt–M/G (M = Ni and Ru) and trimetallic Pt–Ru–Ni/G electrocatalysts were similar, but the peaks of the bimetallic electrocatalysts were less symmetric

than those of Pt–Ru–Ni/G. The higher symmetry of the oxidation peak in the voltammograms of Pt–Ru–Ni/G. The higher symmetry of the oxidation peak in the voltammograms of Pt–Ru–Ni/G suggested that effective, strong electronic interactions took place between the Pt–Ru–Ni nanoparticles and graphene support.

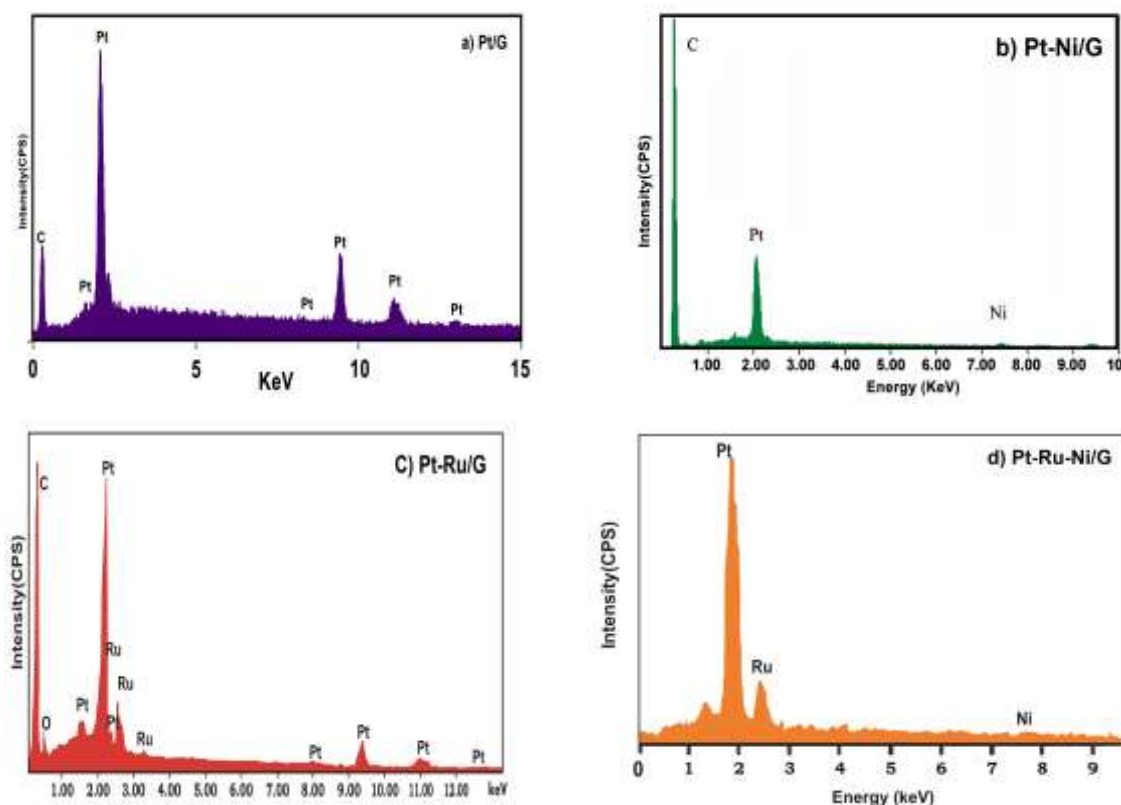


Fig. 5. EDX spectra of a) Pt/G, b) Pt–Ni/G, c) Pt–Ru/G and c) Pt–Ru–Ni/G catalysts

Cyclic voltammetry

Fig. 7a shows the Cyclic Voltammogram (CV) on the Pt/G (100), Pt–Ru/G (50:50), Pt–Ni/G (50:50) and Pt–Ru–Ni/G (60:30:10) catalysts in 0.5 M sulphuric acid solution. The CV curves were obtained in a half cell at a scan rate of 50 mV s^{-1} between 0.05 and +1.2 V (Vs. Ag/AgCl) in the absence of sodium borohydride and it room temperature.

The characteristic features of polycrystalline Pt, i.e. hydrogen adsorption/desorption peak in high potential region, oxide formation/stripping wave/peaks in high potential region and a flat double layer in between, are observed for all the synthesized catalysts. The voltammograms of the electrocatalysts did not display a well-defined hydrogen region between 0.05 and 0.35 V, as the catalyst features in this region are influenced by their surface composition. The binary Pt–Ru/G (50:50), Pt–Ni/G (50:50) catalysts showed a

voltammetric charge similar with reference to that of the pure Pt catalyst. However, a considerable increase in the voltammetric charge of ternary Pt–Ru–Ni/G (60:30:10) catalysts was observed in the double-layer region, indicating that the addition of Ni into binary Pt–Ru/G leads to an enhanced activity for the oxidation reactions. Thus, it can be concluded that the enhanced activity of Pt–Ru–Ni/G (60:30:10) for sodium borohydride electro-oxidation is mainly due to an intrinsic improvement in catalytic activity.

In order to investigate the electrocatalytic activity of the catalysts for sodium borohydride oxidation, the electrochemically active surface area (S_{EAS}) was estimated using different procedures; namely CO adsorption ($S_{EAS/CO}$), hydrogen adsorption/desorption charge ($S_{EAS/H}$), and roughness of electrodes. The S_{EAS} values of the electrocatalysts were calculated by using Eq. (3) and Eq. (4).

$$S_{EAS/H}(m^2/g) = \frac{Q_H(\mu C/cm^2)}{210(\mu C/cm^2) \times 0.77 \times [Pt]} \quad (3)$$

$$S_{EAS/CO}(m^2/g) = \frac{Q_{CO}(\mu C/cm^2)}{420(\mu C/cm^2) \times [Pt]} \quad (4)$$

Where Q_H and Q_{CO} are the charges corresponding to desorption of hydrogen and CO on the Pt surface respectively, $[Pt]$ (mg/cm^2) is the Pt loading on the electrode surface, $210 \mu C/real \text{ cm}^2$ and $420 \mu C/real \text{ cm}^2$ is the charge required to oxidize a monolayer of hydrogen and CO respectively on the Pt surface, 0.77 is the hydrogen monolayer coverage. The roughness of each electrode is calculated by dividing S_{EAS} obtained with the apparent surface area. Estimation of the electrode roughness and S_{EAS} values are shown in Table 2. Based on these values, the highest electrochemically active area is achieved for the ternary electrocatalysts.

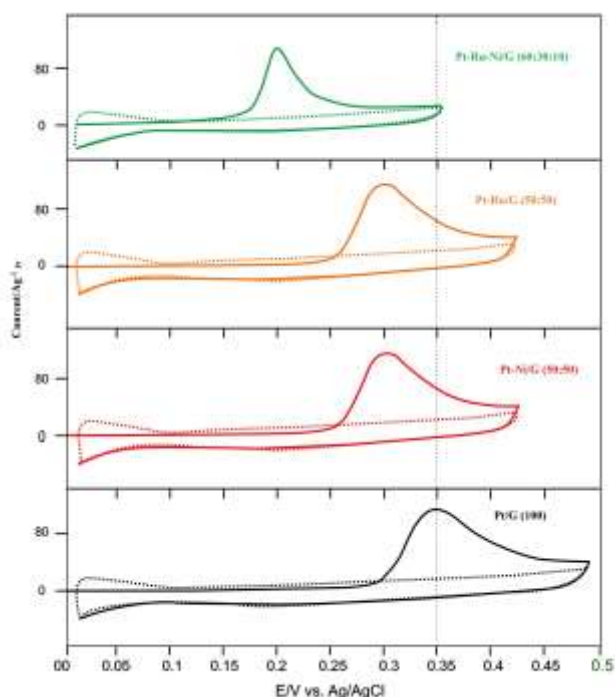


Fig. 6. CO stripping voltammograms of Pt–Ru–Ni/G (60:30:10), Pt–Ru/G (50:50), Pt–Ni/G (50:50) and Pt/G (100) electrocatalysts in $0.5 \text{ M H}_2\text{SO}_4$ at room temperature with a scan rate of 50 mV s^{-1}

Fig. 7.b corresponds to represented cyclic voltammograms of sodium borohydride oxidation under alkali conditions (0.15 M NaBH_4 and 3 M NaOH) catalyzed by Pt–Ru–

Ni/G (60:30:10), Pt–Ru/G (50:50), Pt–Ni/G (50:50), and Pt/G (100) catalysts.

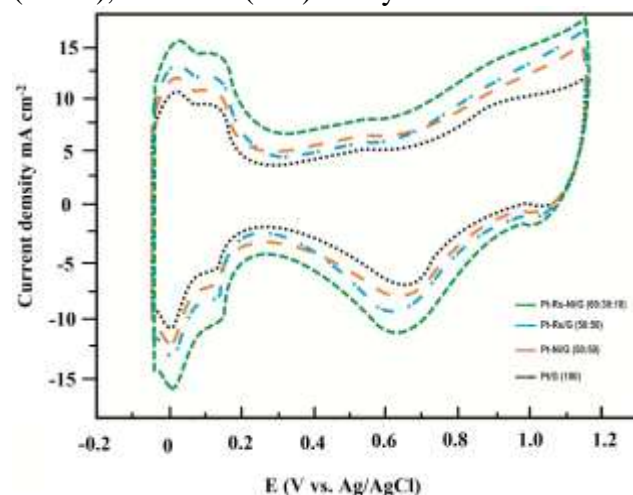


Fig. 7 (a). CVs of Pt–Ru–Ni/G (60:30:10), Pt–Ru/G (50:50), Pt–Ni/G (50:50), and Pt/G (100) catalysts in $0.5 \text{ M H}_2\text{SO}_4$.

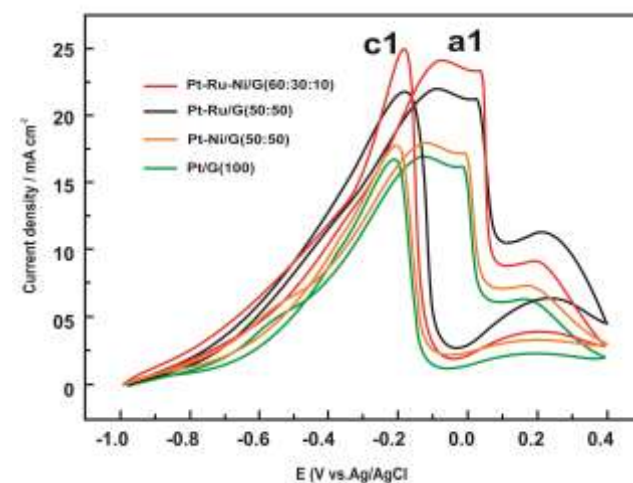


Fig. 7 (b). CVs of Pt–Ru–Ni/G (60:30:10), Pt–Ru/G (50:50), Pt–Ni/G (50:50), and Pt/G (100) catalysts in $0.15 \text{ M NaBH}_4 + 3 \text{ M NaOH}$

In the positive scanning direction in CVs, it can be seen that a wide oxidation peak (a1) appears between -0.6 V and $+0.1 \text{ V}$, which is attributed to the electrooxidation of the intermediate of BH_4^- hydrolysis reaction, i.e. BH_3OH^- . The peak (c1) in the negative scanning direction is also due to BH_3OH^- electro-oxidation, but on the partially oxidized Pt surface. The current density of peak a1 can be employed to evaluate the electrocatalytic activity of the catalysts. The onset potential for the oxidation of sodium borohydride in a positive scan was a significant factor for evaluating the catalyst activity. The onset potentials for the oxidation of sodium borohydride on the Pt–Ru–Ni/G (60:30:10) (-0.97 V) electrocatalysts is slightly lower than that on the Pt–Ru/G (50:50) (-0.93 V), Pt–Ni/G (50:50) (-0.91 V) Pt/G (100)

(–0.89 V) catalysts. The peak current densities of peak a1 on Pt–Ru–Ni/G (60:30:10), Pt–Ru/G (50:50), Pt–Ni/G (50:50), and Pt/G (100) catalysts are 24.98, 22.10, 18.35, and 16.52 mA cm^{–2} respectively. Compared with Pt/G (100) electrocatalyst, the peak current densities of peak (a1) on Pt–Ni/G (50:50), Pt–Ru/G (50:50), and Pt–Ru–Ni/G (60:30:10) electrodes are increased 11.07%, 33.77% and 50.10% respectively,

indicating that the Pt–Ru–Ni/G (60:30:10) electrocatalysts can obviously improve the catalytic activity for BH₄[–] oxidation. Table III summarizes the cyclic voltammogram results of Pt–Ru–Ni/G (60:30:10), Pt–Ru/G (50:50), Pt–Ni/G (50:50), and Pt/G (100) electrocatalysts including the a1 peak of positive peak potential and the peak current densities of BOR.

Table 2. Comparison of hydrogen desorption charge and carbon monoxide desorption charge, and its electrochemical active surface area (S_{EAS}) and electrode roughness

Catalyst	Q _H / μC	Q _{CO} / μC	Electrode real surface area (cm ²)	S _{EAS/H} (m ² gPt ^{–1}) ^a	S _{EAS/CO} (m ² gPt ^{–1}) ^a	Roughness
Pt/G (100)	437	1260	3.0	27	30	90.0
Pt–Ni/G (50:50)	243	735	1.8	30	35	63.0
Pt–Ru/G (50:50)	259	798	1.9	32	38	72.1
Pt–Ru–Ni/G (60:30:10)	417	1184	2.8	43	47	131.5

Table 3. CV results of Pt–Ru–Ni/G (60:30:10), Pt–Ru/G (50:50), Pt–Ni/G (50:50), and Pt/G (100) electrocatalysts at room temperature.

Catalyst	Scan rate 50 mV/s	
	Positive peak potential (V vs. Ag/AgCl)	Peak current density (mA/cm ²)
Pt/G (100)	–0.103	16.52
Pt–Ni/G (50:50)	–0.091	18.35
Pt–Ru/G (50:50)	–0.090	22.10
Pt–Ru–Ni/G (60:30:10)	–0.088	24.98

The CV results show that pure Pt/G (100) catalysts do not behave as an appropriate anode for BOR due to its facile hydrolysis of borohydride. However, the introduction of Ru and Ni promotes the electrocatalysts activity. CV for sodium borohydride oxidation reactions showed that the borohydride hydrolysis was considerably inhibited by Pt–Ru–Ni/G (60:30:10), electrocatalyst, indicating the ability of Ni to promote direct oxidation of sodium borohydride.

Chronoamperometry

The Pt–Ni/G, Pt–Ru/G, and Pt–Ru–Ni/G electrocatalyst performances for borohydride oxidation were studied by chronoamperometry; the potential was stepped from –1.2 to –0.2 V vs. Ag/AgCl, KClstd for 10 minutes, to evaluate the electrocatalytic activity of the catalysts. Fig. 8 shows representative chronoamperograms obtained for the different electrocatalysts whose current densities were normalized by Pt mass. In

the first few minutes, there was a sharp decrease in the current density and after some time, it turn into relatively stable. It can be seen that the current density of sodium borohydride electro-oxidation on the Pt–Ru–Ni/G (60:30:10) catalyst is higher than that on the Pt–Ru/G (50:50), Pt–Ni/G (50:50), and Pt/G (100) catalyst at the same potentials. The activity change for sodium borohydride oxidation decreases in the order of Pt–Ru–Ni/G (60:30:10) > Pt–Ru/G (50:50) > Pt–Ni/G (50:50) > Pt/G (100), which is in fairly good agreement with our CV results for the durability test.

Single cell performance

The Pt/G (100), Pt–Ni/G (50:50), Pt–Ru/G (50:50) and Pt–Ru–Ni/G (60:30:10) catalysts were evaluated as anode catalysts for sodium borohydride electro-oxidation by single membraneless sodium borohydride fuel cell (MLBFC), and the data are presented in Fig 9. When Pt/G (100) was used as the anode catalyst, the performance of single cell was poor. The

open circuit potential (OCP) was 1.68 V, which was mainly attributed to poor catalytic activity towards sodium borohydride electro-oxidation. The maximum output power density for Pt/G (100) is 7.79 mW.cm^{-2} .

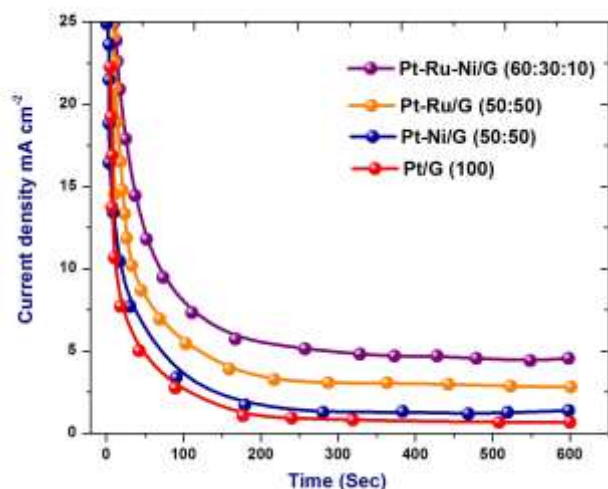


Fig. 8. Chronoamperometry of Pt–Ru–Ni/G (60:30:10), Pt–Ru/G (50:50), Pt–Ni/G (50:50), and Pt/G (100) electrocatalysts

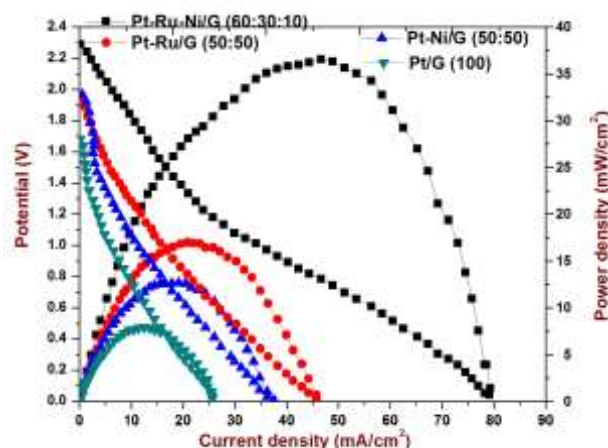


Fig. 9. Polarization and power density curves of different catalyst at 2 mg cm^{-2} catalyst loading on anode and cathode at room temperature. Anode feed: 0.15 M sodium borohydride in 3 M NaOH and Cathode feed: 0.15 M Sodium Perborate + 1.5 M H_2SO_4

The addition of Ru is considerably decreasing the sodium borohydride electro-oxidation reaction as observed from the polarization curves. The Ru content that provides maximum activity is in the range 30 at % of Ru: a decrease in the BOR activity for higher Ru contents is commonly ascribed to hindering access of the reactant to Pt sites by the presence of Ru oxide and/or low amounts of Pt sites; lower Ru contents depend on the degree of alloying. Above 30 at %, alloyed Ru hinders sodium borohydride adsorption by the ensemble

effect. On these bases, the best compromise alloyed Ru in Pt–Ru/G catalysts should be 20–30 at %. Pt–Ru/G (50:50) (Ru 50 at %) and Pt–Ru–Ni/G (60:30:10) (Ru 30 at.%) showed OCP of 1.94 V and 2.28V respectively. The comparison of both the bimetallic catalysts showed that peak power density of Pt–Ru/G (50:50) (16.99 mW.cm^{-2}). The results of MLBFC adapting to different catalysts are illustrated in Fig. 10.

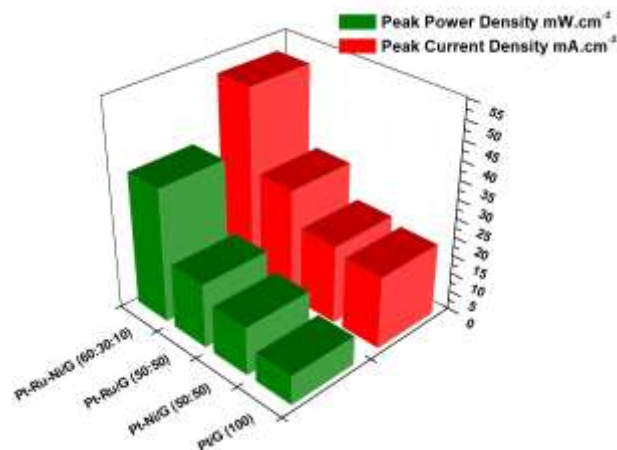


Fig. 10 Peak current density and peak power density of Pt–Ru–Ni/G (60:30:10), Pt–Ru/G (50:50), Pt–Ni/G (50:50), and Pt/G (100) electrocatalysts at room temperature. Anode feed: 0.15 M sodium borohydride in 3 M NaOH and Cathode feed: 0.15 M Sodium Perborate + 1.5 M H_2SO_4 . Stream flow rates: 0.3 ml min^{-1}

When the current was standardized to the geometric area of single cell, it was observed that the cell performance of Pt–Ru–Ni/G (60:30:10) catalyst was better than other catalysts. In the low current discharging region, the power drawn from single cell was almost the same for all catalysts except Pt–Ru/G (50:50) and Pt/G (100). The cell voltage of Pt–Ru–Ni/G (60:30:10) at a current density of 51.21 mA cm^{-2} was 0.69 mV which was higher than rest of the catalyst. In addition, there was a rapid initial fall in cell voltage for all catalysts, which was due to the slow initial sodium borohydride electro-oxidation reaction at the electrode surface. After an initial drop of 0.69 mV the change in slope of the polarization curve for Pt–Ru–Ni/G (60:30:10) decreased, and it started drawing more current. This is attributed to the more effective catalytic ability of Pt–Ru–Ni/G (60:30:10), once the sodium borohydride electro-oxidation reaction being initiated. Based on the power density drawn from single cell, Pt–Ru–Ni/G (60:30:10) is the best anode catalyst

with peak power density value of 35.61 mW.cm⁻².

Conclusions

The colloidal metals Pt–Ru, Pt–Ni, and Pt–Ru–Ni supported on graphene were prepared by bonnemann method and investigated as electrocatalysts for borohydride electro-oxidation. A uniform dispersion of the catalytic particles on the graphene support is achieved, and most of the Ru and Ni are found as unalloyed oxides on the surface of nanoparticles as revealed by XRD analyses. The TEM images indicated an average particle size of Pt–Ru–Ni/G (60:30:10) nanoparticle of 3–4 nm. EDX reveals that the Ni content is lower than the nominal value. The catalytic activity was assessed by cyclic voltammetry and chronoamperometry. The maximum activity for sodium borohydride oxidation was found for the Pt–Ru–Ni/G (60:30:10) than the Pt–Ru/G (50:50), Pt–Ni/G (50:50) and Pt/G (100) catalysts. The significantly enhanced catalytic activity for sodium borohydride oxidation can be attributed to the high dispersion of ternary catalysts and to Ni acting as a promoting agent. The MLBFC employing Pt–Ru–Ni/G (60:30:10) as anode catalyst and Pt/G as cathode catalyst obtained the maximum power density is 35.61 mW/cm² at room temperature. From the electrochemical tests and single cell test, the graphene-supported Pt–Ru–Ni (60:30:10) catalysts offer the potential to be considered as an alternative anode catalyst for MLBFCs.

Conflict of interest

Authors declare there are no conflicts of interest.

References

- [1] Duteanu N, Vlachogiannopoulos G, Shivhare MR, Yu EH, Keith S, A parametric study of a platinum ruthenium anode in a direct borohydride fuel cell, *J Appl Electrochem.* 2007; 37(9): 1085–1091.
- [2] Tegou A, Papadimitriou S, Mintsouli I, Armyanov S, Valova E, Kokkinidis G, Rotating disc electrode studies of borohydride oxidation at Pt and bimetallic Pt–Ni and Pt–Co electrodes. *Catal Today*, 2011; 170(1): 126–33.
- [3] Yi LH, Liu L, Liu X, Wang XY, Yi W, He PY, Carbon supported Pt–Co nanoparticles as anode catalyst for direct borohydride-hydrogen peroxide fuel cell: electrocatalysts and fuel cell performance. *Int. J. Hydrogen Energy*, 2012; 37(17): 12650–12658.
- [4] Gowdhamamoorthi M, Arun A, Kiruthika S and Muthukumaran B. Percarbonate as novel fuel for enhanced performance of membraneless fuel cells. *Int. J. of Ionics* 2014; 20(12): 1723–1728.
- [5] Arun A, Gowdhamamoorthi M, Kiruthika S and Muthukumaran B. Analysis of membraneless methanol fuel cell using percarbonate as an oxidant. *J. of the Electrochemical Society*, 2013; 161: F1–F7.
- [6] Yi LH, Liu L, Wang XY, Liu X, Yi W, Wang XY. Carbon supported Pt–Sn nanoparticles as anode catalyst for direct borohydride-hydrogen peroxide fuel cell: electrocatalysis and fuel cell performance. *J Power Sources*, 2013; 224: 6–12.
- [7] Yi LH, Hu B, Song YF, Wang XY, Zou GS, Yi W, Studies of electrochemical performance of carbon supported Pt–Cu nanoparticles as anode catalysts for direct borohydride hydrogen peroxide fuel cell, *J Power Sources* 2011; 196(23): 9924–30.
- [8] Elumalai M, Priya M, Kiruthika S, Muthukumaran B, Effect of acid and alkaline media on membraneless fuel cell using sodium borohydride as a fuel, *J. Afinidad* 2015; 72: 572.
- [9] Yang H, Coutanceau C, Leger JM, Alonso-Vante N, Lamy C, Methanol tolerant oxygen reduction on carbon-supported Pt–Ni alloy nanoparticles, *J. Electroanal. Chem.* 2005; 576(2): 305–313.
- [10] Lobato J, Ca nizares P, Rodrigo MA, Linares JJ, Lopez-Vizcaino R, Performance of a Vapor-Fed Polybenzimidazole (PBI)-Based Direct Methanol Fuel Cell, *J. of Energy Fuels*, 2008; 22(5):3335–3345.
- [11] Hsieh CT, Lin JY, Fabrication of bimetallic Pt–M (M= Fe, Co, and Ni) nanoparticle/carbon nanotubes electrocatalysts for direct methanol fuel cells, *J. Power Sources* 2009; 188(2): 347–352.
- [12] Lobato CJ, Ca nizares P, Ubeda D, Pinar FJ, Rodrigo MA, Testing PtRu/CNF catalysts for a high temperature polybenzimidazole-based direct ethanol fuel cell. Effect of metal content, *Appl. Catal. B: Environ.* 2011; 106(2): 174–180.

- [13] Yaojuan H, Ping W, Yajing Y, Hui Z, Chenxin C, Effects of structure, composition, and carbon support properties on the electrocatalytic activity of Pt-Ni-graphene nanocatalysts for the methanol oxidation, *Applied Catalysis B: Environmental*, 2012; 111: 208–217.
- [14] John S.St, Dutta I, Angelopoulos A.P, Enhanced Electrocatalytic Oxygen Reduction through Electrostatic Assembly of Pt Nanoparticles onto Porous Carbon Supports from SnCl₂-Stabilized Suspensions, *Langmuir*, 2011; 27(10): 5781–5791.
- [15] Qi J, Jiang L, Wang S, Sun G, Synthesis of graphitic mesoporous carbons with high surface areas and their applications in direct methanol fuel cells, *Appl. Catal. B: Environ.* 2011; 107(2): 95–103.
- [16] Yang H, Li F, Shan C, Han D, Zhang Q, Niu L, Ivaska A, Covalent functionalization of chemically converted graphene sheets via silane and its reinforcement, *J. Mater. Chem.* 2009; 19(26): 4632–4638.
- [17] Kou R, Shao Y, Mei D, Nie Z, Wang D, Wang C, Viswanathan VV, Park S, Aksay IA, Lin Y, Wang Y, Liu J, Stabilization of Electrocatalytic Metal Nanoparticles at Metal-Metal Oxide-Graphene Triple Junction Points, *J. Am. Chem. Soc.* 2011; 133(8): 2541–2547.
- [18] Yang F, Liu Y, Gao L, Sun J, pH-Sensitive Highly Dispersed Reduced Graphene Oxide Solution Using Lysozyme via an in Situ Reduction Method, *J. Phys. Chem. C*, 2010; 114(50): 22085–22091.
- [19] Ermete A, Effect of the Structural Characteristics of Binary Pt–Ru and Ternary Pt–Ru–M Fuel Cell Catalysts on the Activity of Ethanol Electro-oxidation in Acid Medium. *ChemSusChem*. 2013; 6(6): 966-973.
- [20] Lam VW S, Alfantazi A, Gyenge EL, The effect of catalyst support on the performance of PtRu in direct borohydride fuel cell anodes, *J Appl Electrochem.* 2009; 39:1763–1770.
- [21] Martinez-Huerta MV, Rojas S, Fuente JLG, Terreros P, Pena MA, Fierro JLG, Effect of Ni addition over PtRu/C based electrocatalysts for fuel cell applications, *Appl. Catal. B: Environ.* 2006; 69(2): 75–84.
- [22] Moreno B, Chinarro E, Perez JC, Jurado JR, Combustion synthesis and electrochemical characterization of Pt–Ru–Ni anode electrocatalyst for PEMFC, *Appl. Catal. B: Environ.* 2007; 76(3): 368–374.
- [23] Gotz M, Wendt H, Binary and ternary anode catalyst formulations including the elements W, Sn and Mo for PEMFCs operated on methanol or reformat gas. *Electrochimica Acta*, 1998; 43(24): 3637-3644.
- [24] Radmilovic V, Gasteiger HA, Ross Jr. PN, Structure and chemical composition of a supported Pt-Ru electrocatalyst for methanol oxidation, *J. Catal.* 1995; 154(1): 98-106.
- [25] Beyhan S, Leger J-M, Kadirgan F, Pronounced synergetic effect of the nano-sized PtSnNi/C catalyst for methanol oxidation in direct methanol fuel cell, *Applied Catalysis B: Environmental* 2013; 130: 305–313.
- [26] Giorgi L, Pozio A, Bracchini C, Giorgi R, Turtu S, H₂ and H₂/CO oxidation mechanism on Pt/C, Ru/C and Pt–Ru/C electrocatalysts, *J. Appl. Electrochem.* 2001; 31(3) 325-334.
- [27] Wang ZB, Yin GP, Shi PF, Sun YC, Novel Pt–Ru–Ni/C Catalysts for Methanol Electro-oxidation in Acid Medium, *Electrochem. Solid-State Lett.* 2006; 9(1): A13.
